REPORT A69-2

STRAIN GAGE INSTRUMENTATION FOR A LIGHT GAS GUN

by

P. D. FLYNN

May 1969

DEPARTMENT OF THE ARMY
FRANKFORD ARSENAL
Philadelphia, Pa. 19137

REPORT A69-2

STRAIN GAGE INSTRUMENTATION FOR A LIGHT GAS GUN

by

P. D. FLYNN

AMCMS Code 5011.11.85804
DA Project 1T061102B33A04

Pitman-Dunn Research Laboratories
FRANKFORD ARSENAL
Philadelphia, Pa. 19137

May 1969

PREFACE

This paper was presented at the IEEE (3rd) International Congress on Instrumentation in Aerospace Simulation Facilities held at the Polytechnic Institute of Brooklyn Graduate Center, Farmingdale, N. Y., 5-8 May 1969. It was published by the Institute of Electrical and Electronic Engineers, Inc., New York, N. Y., in the Congress Record, May 1969, pp. 184-189.

STRAIN GAGE INSTRUMENTATION FOR A LIGHT GAS GUN

P. D. Flynn
Pitman-Dunn Research Laboratories
Frankford Arsenal, Philadelphia, Pa., U.S.A.

ABSTRACT

Variable-resistance strain gages were used to study the operating characteristics of a light-gas gun. Gages were cemented on the outer surface of the gun at several locations in order to determine chamber pressure, piston velocity, and pressures in the central breech. The high-pressure transition section deformed plastically in most rounds, and a method is suggested for estimating maximum pressures from strain-time records. Results are given for various helium pressures and powder charges.

INTRODUCTION

The velocity limitations of conventional guns are well known.[1] Various methods have been used to obtain higher velocities, and light-gas guns are in rather widespread use.[2] The Physics Research Laboratory recently completed installation of a piston-compression light-gas gun in its hypervelocity test facility. In order to optimize the performance of the gun in the range of projectile impacts of interest to Frankford Arsenal, strain gage instrumentation was developed to monitor the dynamic behavior of the gun. The purpose of this paper is to describe the techniques which were used and to present typical results which suggest the potential usefulness of strain gages in this field.

TEST PROCEDURES

Experimental Setup. Figure 1 gives an overall view of the light-gas gun and hypervelocity test facility which can be used to fire projectiles in controlled atmospheres from high vacuum to 100 psig. All firings reported in this paper were made into air at 10 mm of mercury absolute pressure. The first section of the light-gas gun consisted of a 40 mm breech mechanism, chamber and barrel from a surplus naval anti-aircraft gun. The barrel was modified so that it could be coupled to a pump tube (56 in. long, 4.00 in. OD, 1.63 in. ID). Fittings were installed on the pump tube so that the gun could be evacuated and a light gas introduced. Helium was used in these tests. An 18 in. long section was used between the pump tube and the central breech or high-pressure transition section. The high-pressure section (13 in. long, 7 in. OD) provided the transition from the 1.63 in. ID pump tube to a caliber .60, smooth-bore launch tube (75 in. long). After completing the tests reported in this paper, the central breech was sectioned and photographed, Fig. 2. This figure also shows a projectile (steel cube, 10 grains), carrier (aluminum, 87 grains), shear disk (aluminum, 0.020 in. thick), disassembled lexan piston and steel slug (total weight 820 grams), and a 40 mm shell used in a typical firing.

Strain Gages. Budd[3] Type 364-1000 strain gages were selected because they have a high gage factor (F = 3.26) and a high resistance (R = 1000 Ω)

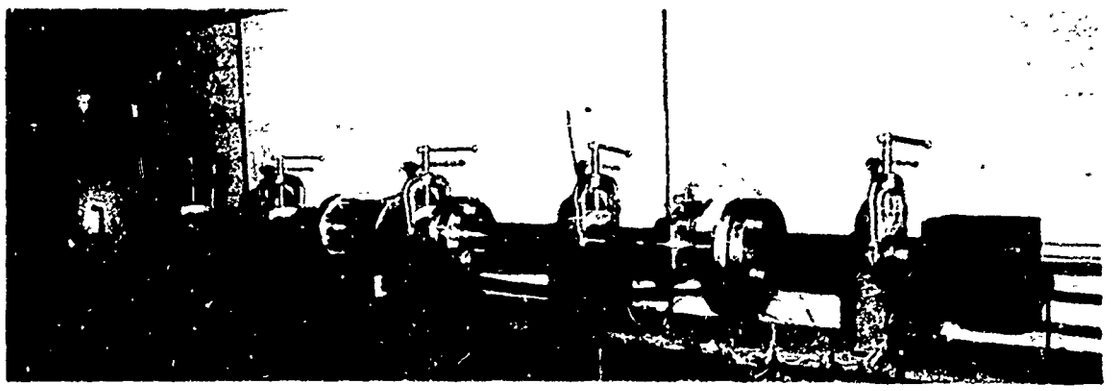

Fig. 1 Light Gas Gun and Hypervelocity Test Facility

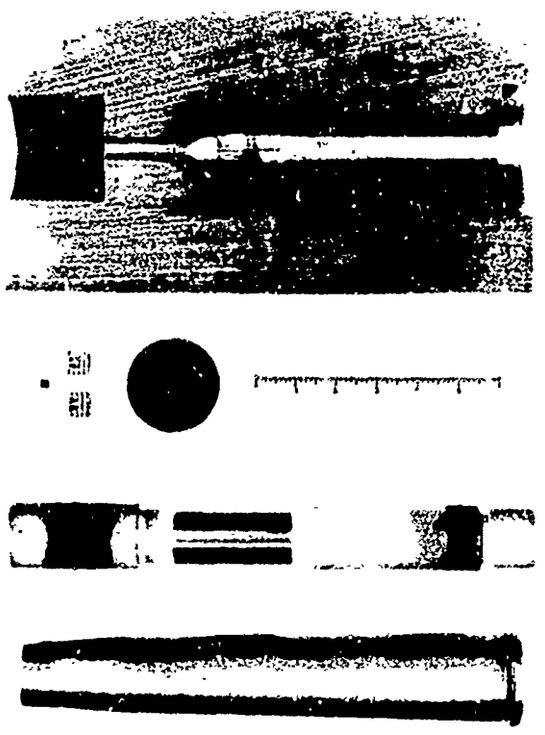

Fig. 2 Central Breech after Sectioning and Components used in Gun

so that relatively large output signals were obtained. Chamber pressures were determined from circumferential and longitudinal strain gages, $(\epsilon_\theta)_{P1}$ and $(\epsilon_z)_{P1}$, cemented on the outer surface of the barrel at pressure station P1 midway between the breech and first clamp. An average piston velocity was obtained from circumferential strains, $(\epsilon_\theta)_{V1}$ and $(\epsilon_\theta)_{V2}$, at velocity stations V1 and V2 on the pump tube, 12 in. apart, symmetrically placed with respect to the second clamp. Strains $(\epsilon_\theta)_{P2}$ and $(\epsilon_z)_{P2}$ were measured on the outer surface of the high-pressure section at pressure station P2 which was located 2 in. before the internal transition from 1.63 in. to caliber .60. The strain gages and wiring can be seen in Fig. 1.

A potentiometer circuit, Fig. 3, was used to measure dynamic strains, and although the principle of operation is well known,[4] the essential features are given here for completeness. From Ohm's law, the voltage drop across the gage, V_g, is

$$V_g = V R_g/(R_b+R_g) \qquad (1)$$

where V is the constant power supply voltage, R_g is the gage resistance, and R_b is the ballast resistance. Differentiating with respect to R_g we obtain

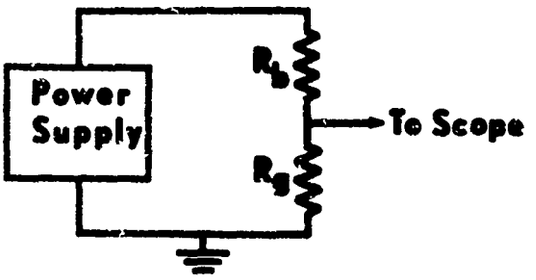

Fig. 3 Potentiometer Circuit for Dynamic Strains

$$\frac{dV_g}{dR_g} = \frac{V R_b}{(R_b+R_g)^2} \qquad (2)$$

The change in gage resistance depends on the strain, ϵ, and the manufacturer's gage factor, F, is defined such that

$$\Delta R_g/R_g = F \epsilon \qquad (3)$$

For small values of $\Delta R_g/R_g$ we obtain from Eqs. (2) and (3)

$$\Delta V_g = \frac{V}{R_b+R_g} \cdot \frac{R_b}{R_b+R_g} \cdot R_g F \epsilon \qquad (4)$$

and from Eqs. (4) and (1), we obtain

$$\epsilon = \frac{1+R_g/R_b}{F} \cdot \frac{\Delta V_g}{V_g} \qquad (5)$$

Dynamic strains were determined by measuring the voltage change, ΔV_g, as a function of time.

In each circuit, two gages were used in series (R_g = 2000 Ω) to increase the output and to average the surface strains at each location. Four potentiometer circuits were connected in parallel across a laboratory power supply with ballast resistors of about 7500 Ω each for the strains $(\epsilon_\theta)_{P1}$, $(\epsilon_z)_{P1}$, $(\epsilon_\theta)_{V1}$, and $(\epsilon_\theta)_{V2}$. Altec[5] constant current sources were used for $(\epsilon_\theta)_{P2}$ and $(\epsilon_z)_{P2}$, and for these strains, Eq. (5) reduces to

$$\epsilon = \frac{1}{F} \cdot \frac{\Delta V_g}{V_g} \qquad (5a)$$

The outputs of the strain gage circuits were recorded on two Tektronix dual-beam oscilloscopes using various plug-in units.

Tube with Internal Pressure. From Lame's solution, the circumferential and radial stresses, σ_θ and σ_r, in an elastic thick-walled cylinder subjected to static internal pressure, p, are[6]

$$\sigma_\theta = \frac{a^2 p}{b^2-a^2}(1 + b^2/r^2) \qquad (6a)$$

$$\sigma_r = \frac{a^2 p}{b^2 - a^2}\left(1 - b^2/r^2\right) \qquad (6b)$$

where a and b are the inner and outer radii as shown in Fig. 4. The axial stress, σ_z, depends on the end conditions.

At the outer surface, r=b, so that

$$\sigma_\theta = 2a^2 p/(b^2 - a^2)$$
$$\sigma_r = 0 \qquad (7)$$

From Hooke's law, the strains on the outer surface are given by

$$\epsilon_\theta = (\sigma_\theta - \mu\sigma_z)/E$$
$$\epsilon_z = (\sigma_z - \mu\sigma_\theta)/E \qquad (8)$$

where E is Young's modulus and μ is Poisson's ratio, so that the stresses in terms of the strains are

$$\sigma_\theta = E(\epsilon_\theta + \mu\epsilon_z)/(1-\mu^2)$$
$$\sigma_z = E(\epsilon_z + \mu\epsilon_\theta)/(1-\mu^2) \qquad (9)$$

From Eqs. (7) and (9), and introducing the wall ratio, w = b/a, we obtain

$$p = \frac{w^2 - 1}{2} \cdot \frac{E}{1-\mu^2} \cdot (\epsilon_\theta + \mu\epsilon_z) \qquad (10)$$

Hence the static internal pressure, p, can be determined by measuring the strains, ϵ_θ and ϵ_z, on the outer surface of an elastic thick-walled cylinder.

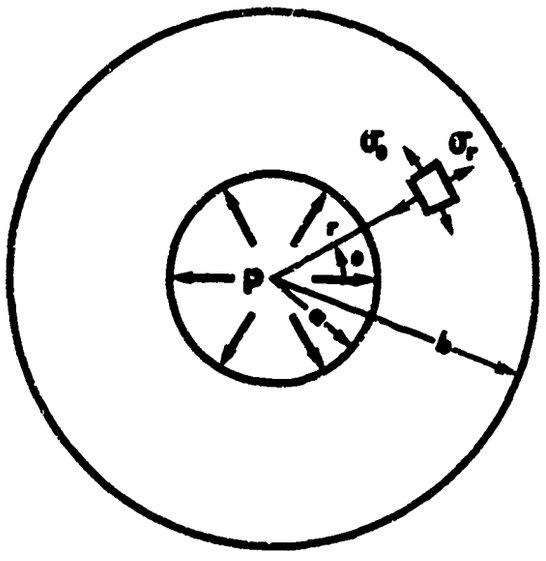

Fig. 4 Thick-Walled Tube with Internal Pressure

Equation (10) can be used to calculate ballistic pressures so long as the loading is quasi-static, the material responds elastically, and the gun approximates a thick-walled cylinder. It will be shown that these conditions were met reasonably well at the chamber. However, the high-pressure section deformed plastically, and a modified form of Eq. (10) will be suggested later for estimating the maximum pressure produced during compression of the helium and impact of the piston.

Range Instrumentation. Two independent systems were used to measure projectile velocities. One system used flash X-rays, and the other employed a photo-optical system with two slit images which were recorded by a Fastax streak camera. During each test the streak camera was started first, and a synchronizing pulse was obtained after counting a preset number of sprocket teeth. The synchronizing pulse triggered the oscilloscopes and ignited an electric primer which shot a firing pin against a mechanical primer in the round. Since some difficulties were encountered in launching the projectiles and in synchronizing the flash X-rays, projectile velocity data have been omitted from this paper.

RESULTS AND DISCUSSION

Seven preliminary rounds were fired in which the piston configuration changed from an all lexan design (21 in. long) to short lexan pistons weighted with cerrobend (a low melting bismuth alloy), lead, or steel. Several types of carriers were used, and the helium pressure and propellant charge were varied.

For the tests reported in this paper, a new high-pressure section was installed, and the components shown in Fig. 2 were similar throughout these tests. Table 1 lists the helium pressures and powder charges used in Rounds 8-14. The high-pressure section was measured before and after each test, and the outside and inside diameters at strain gage station P2 are listed in Table 1.

Table 1 Schedule of Tests

Round	Helium Pressure psia	Powder Charge grams	Diameters at P2 OD in.	Diameters at P2 ID in.
			6.948	1.628
8	300	227	6.953	1.653
9	200	227	6.961	1.685
10	100	227	6.975	1.723
11	300	227	6.976	1.727
12	500	227	6.976	1.727
13	300	159	6.976	1.727
14	300	318	6.995	1.776

Measurements were also made on the chamber, pump tube and 18 in. section, and the light-gas gun was dimensionally stable except at the high-pressure section.

Strain Gage Records. Figure 5A shows typical strain versus time traces for all gages except $(\epsilon_z)_{P2}$ in Round 11. The slight disturbances on the left-hand side of these traces were due to the synchronizing or firing pulse, and fortunately these initial disturbances decayed rapidly and did not affect the strain gage records. The circumferential strain $(\epsilon_\theta)_{P1}$ increased rather smoothly and appeared to be similar to a pressure-time curve. The longitudinal strain $(\epsilon_z)_{P1}$ increased too, but high frequency oscillations due to longitudinal waves in the gun were superimposed on this trace. Both the $(\epsilon_\theta)_{V1}$ and $(\epsilon_\theta)_{V2}$ traces exhibited a sudden increase as the piston moved past the velocity stations on the pump tube. These traces were recorded on a second oscilloscope, Fig. 5B, using a delayed and faster sweep in order to obtain a more accurate measure of the piston velocity. The circumferential strain $(\epsilon_\theta)_{P2}$ on the high-pressure section was also recorded on two oscilloscopes, Figs. 5A,B. Impact of the piston produced rather large longitudinal and circumferential strains in the gun as seen at later times on the traces in Fig. 5A, e.g., $(\epsilon_z)_{P1}$ increased abruptly and went off scale whereas $(\epsilon_\theta)_{P1}$ decreased sharply because of coupling through Poisson's ratio.

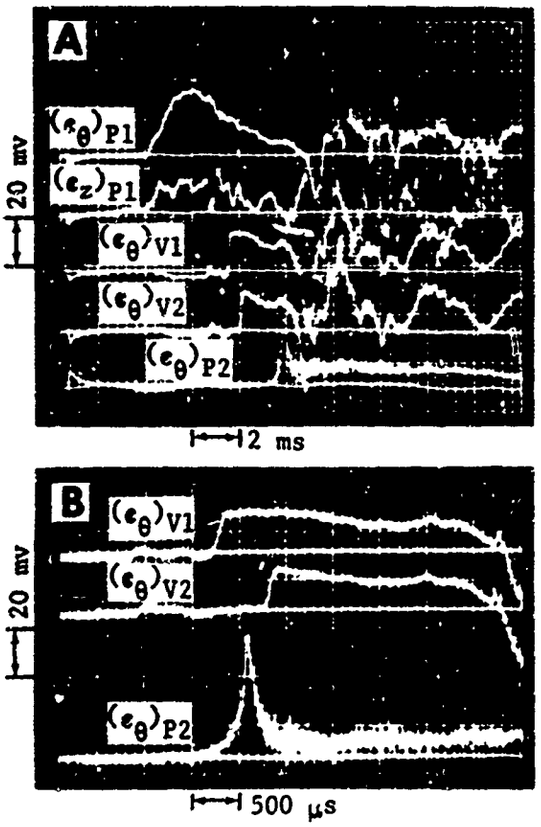

Fig. 5 Typical Strain-Time Traces, Round 11

Piston Velocity. As previously noted, strain gages were mounted circumferentially at two stations on the pump tube, 12 in. apart, symmetrically placed with respect to the second clamp. Average piston velocities were calculated by dividing this base line by the time interval between the rises in the $(\epsilon_\theta)_{V1}$ and $(\epsilon_\theta)_{V2}$ traces, Table 2. Although these piston velocities were not the maximum values in the pump tube, it is interesting to note that the average values obtained at this location were independent of helium pressure and varied linearly with charge.

Chamber Pressure. The strains $(\epsilon_\theta)_{P1}$ and $(\epsilon_z)_{P1}$ were used in Eq. (10) to calculate maximum chamber pressures, Table 2. Since the $(\epsilon_\theta)_{P1}$ traces were relatively smooth curves, the maximum values were obtained easily. The corresponding values of $(\epsilon_z)_{P1}$ were obtained by ignoring the oscillations and estimating its mean values. The error introduced in Eq. (10) by using this procedure was small because $(\epsilon_z)_{P1}$ was multiplied by Poisson's ratio (μ=0.3) and $(\epsilon_z)_{P1}$ was less than $(\epsilon_\theta)_{P1}$. Pressures were transmitted through the shell to the barrel, and the wall ratio was w=OD/ID=4.322/1.933 at the strain gages. The maximum chamber pressures were independent of helium pressure and increased rapidly with increasing charge. A standard charge of 318 grams of SPDN 8709 powder when used with a standard 40 mm projectile weighing 890 grams has a chamber pressure of 43,900 psi. Using the same charge and a piston of 820 grams, a pressure of 40 kpsi was obtained in the light-gas gun, and this value compares favorably with the gated chamber pressure.

High-Pressure Section. The pressures developed in the central breech during Rounds 8-11,14 produced permanent deformations, Table 1. The residual circumferential strain, $(\epsilon_\theta)_{res}$ at the outer surface was calculated from the change in diameter, Δ(OD), i.e.,

Table 2 Piston Velocities and Chamber Pressures

Round	Piston Velocity ft/sec	Maximum Chamber Pressure $(\epsilon_\theta)_{P1}$ με	$(\epsilon_z)_{P1}$ με	p kpsi
8	1600	201	10[illegible]	15
9	1700	186	93	14
10	1700	186	93	1[illegible]
11	1800	201	108	15
12	1700	186	93	14
13	1300	77	54	6
14	2500	542	194	40

$$(\epsilon_\theta)_{res} = \frac{\delta(OD)}{OD} \qquad (11)$$

for each round, Table 3. The strain-time records of $(\epsilon_\theta)_{P2}$ also gave values of $(\epsilon_\theta)_{res}$ as shown in Fig. 6 and listed in Table 3. It should be noted that a change in outside diameter of 0.001 in. corresponded to 340 με, so that under these circumstances the values of $(\epsilon_\theta)_{res}$ obtained by these two methods were in fairly good agreement.

Since the high-pressure section deformed plastically, Eq. (10) was not applicable. Measurements of $(\epsilon_z)_{P2}$ showed that it was small compared to $(\epsilon_\theta)_{P2}$. In order to estimate that maximum pressure, $(\epsilon_z)_{P2}$ was neglected in Eq. (10) and $(\epsilon_\theta)_{P2}$ was replaced by $(\epsilon_\theta)_{el}$ as defined in Fig. 6 i.e.,

$$P_{max} = \frac{w^2-1}{2} \cdot \frac{E}{1-\mu^2} \cdot (\epsilon_\theta)_{el} \qquad (12)$$

The p vs. $(\epsilon_\theta)_{P2}$ behavior of the tube is shown in Fig. 7, assuming a linear recovery from P_{max}. The slope of this line, i.e ,

$$S = \frac{w^2-1}{2} \cdot \frac{E}{1-\mu^2} \qquad (13)$$

was calculated using values of $E = 30 \times 10^6$ psi and $\mu = 0.3$ for steel and w based on the dimensions

Table 3 Residual Strains and Maximum Pressures

Round	Micrometer $(\epsilon_\theta)_{res}$ με	Strain Gages, $(\epsilon_\theta)_{P2}$ $(\epsilon_\theta)_{res}$ με	$(\epsilon_\theta)_{el}$ με	P_{max} ksi
8	720	840	1080	300
9	1150	1210	1460	370
10	2010	1800	2410	610
11	140	240	1260	320
12	0	0	840	210
13	0	0	510	130
14	2720	3040	3340	800

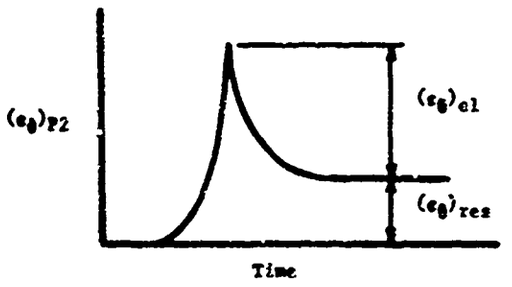

Fig. 6 Sketch of $(\epsilon_\theta)_{P2}$ vs. Time

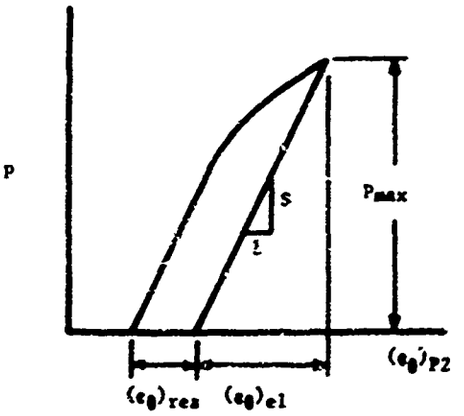

Fig. 7 Sketch of p vs. $(\epsilon_\theta)_{P2}$

after each test. The values of P_{max} calculated in this way are listed in Table 3 and plotted in Fig. 8. For the same helium pressure and powder charge in Rounds 8 and 11, it is interesting to note that this procedure gave approximately the same values of P_{max} even though the high-pressure section had been rather severely overstrained in Rounds 8-10 and was nearly stable dimensionally in Round 11. Although the data in Fig. 8 are very limited, it appears that this type of graph will be useful in selecting operating conditions for the light-gas gun.

Assuming an elastic-plastic material and the maximum shear theory of yielding, it can be shown[7] that a thick-walled cylinder becomes fully plastic at a pressure, P_{ult}, given by

$$P_{ult} = \sigma_{yp} \cdot \ln w \qquad (14)$$

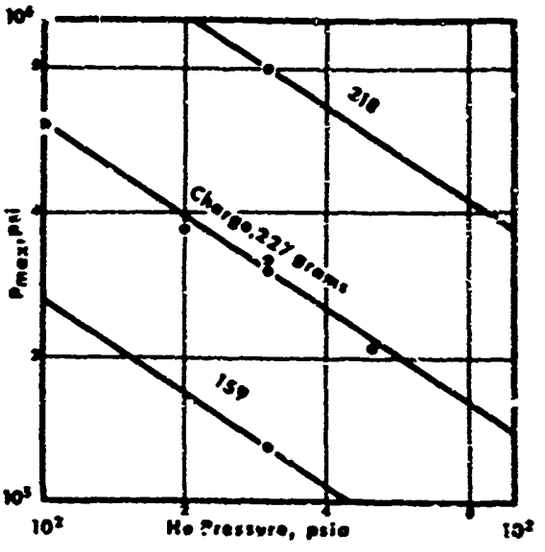

Fig. 8 P_{max} vs. Helium Pressure

where σ_{yp} is the tensile yield point of the material. The high-pressure section was made of 4340 steel, Rockwell C30, with σ_{yp} = 120,000 psi. Using the initial dimensions, i.e., w = 6.948/1.628, we obtain p_{ult} = 174,000 psi. Rounds 12 and 13 were the only rounds in this series of tests which did not introduce additional permanent deformations, and the values of p_{max} were comparable to p_{ult}. Rounds 8,9,11 gave somewhat higher pressures as would be expected. Assuming that the values of p_{max} for Rounds 8,9,11,12,13 are reliable, extrapolation of these data as in Fig. 8 would indicate that the rather high pressures calculated for Rounds 10 and 14 by using Eq. (12) are reasonable values.

CONCLUDING REMARKS

Strain gages provided valuable information on the operating characteristics of the light-gas gun They were cemented on the outer surface so that the gun was not weakened by drilling and tapping as is usually done for pressure gages and velocity probes. However, the output of a strain gage is generally only an indirect measure of some ballistic parameter of interest. In the present work, the interpretation was relatively straight-forward for piston velocities and chamber pressures, whereas the calculations for maximum pressures in the high-pressure section involved several simplifying assumptions. Equation (12) seems to give reasonable values of p_{max} and Fig. 8 appears to be a useful way of comparing various operating conditions of the gun. Further experimental and theoretical work is needed to determine the range of applicability of the proposed method for calculating p_{max}.

ACKNOWLEDGMENTS

It is a pleasure to acknowledge the cooperation and technical assistance of J.T. Gilbert in all phases of this work. Sincere thanks are expressed to the following: J.P. Shields and E.A. Webster, Jr. conducted the firings in the hypervelocity test facility, J.R. Revell performed all of the required machining, and J.A. Brittain measured critical sections of the gun. This work was undertaken at the request of the Hyperdynamics Branch, and the helpful discussions and encouragement received from L.F. Baldini, H.E. Fatzinger, and J.R. Kymer are gratefully acknowledged.

REFERENCES

1. Seigel, A.E. The Theory of High Speed Guns, North Atlantic Treaty Organization, Advisory Group for Aerospace Research and Development, AGARDograph 91, May 1965.

2. Swift, H.F. "Hypervelocity Ballistic Accelerators," Proc. 5th Symposium on Hypervelocity Impact, Denver 1961, Vol. 1 - Part 1, April 1962, pp. 1-22.

3. Automation Industries, Inc., P.O. Box 245, Phoenixville, Pa. Budd Metalfilm Strain Gages and Accessories, Catalog BG24CO/B.

4. Dove, R.C. and Adams, P.H. Experimental Stress Analysis and Motion Measurement, C.E. Merrill Books, Columbus, 1964, p.92.

5. Altec, 5407 Acoma Rd., SE, Albuquerque, New Mexico. Constant Current Source, Model 103.

6. Timoshenko, S. and Goodier, J.N. Theory of Elasticity, 2nd ed., McGraw-Hill, New York, 1951, p.60.

7. Timoshenko, S. Strength of Materials, Part II, 3rd ed., Van Nostrand, Princeton, 1956, p.386.

UNCLASSIFIED

Security Classification

DOCUMENT CONTROL DATA - R & D

(Security classification of title, body of abstract and indexing annotation must be entered when the overall report is classified)

1. ORIGINATING ACTIVITY (Corporate author)	2a. REPORT SECURITY CLASSIFICATION
FRANKFORD ARSENAL Philadelphia, Pa. 19137	Unclassified
	2b. GROUP N/A

3. REPORT TITLE

STRAIN GAGE INSTRUMENTATION FOR A LIGHT GAS GUN

4. DESCRIPTIVE NOTES (Type of report and inclusive dates)

Technical Research Article

5. AUTHOR(S) (First name, middle initial, last name)

P. D. FLYNN

6. REPORT DATE	7a. TOTAL NO. OF PAGES	7b. NO. OF REFS
May 1969	11	7

8a. CONTRACT OR GRANT NO.	9a. ORIGINATOR'S REPORT NUMBER(S)
AMCMS Code 5011.11.85804 b. PROJECT NO. DA Project 1T061102B33A04 c. d.	Report A69-2 9b. OTHER REPORT NO(S) (Any other numbers that may be assigned this report)

10. DISTRIBUTION STATEMENT

This document has been approved for public release and sale; its distribution is unlimited.

11. SUPPLEMENTARY NOTES	12. SPONSORING MILITARY ACTIVITY
	AMSMU-RE-B

13. ABSTRACT

Variable-resistance strain gages were used to study the operating characteristics of a light-gas gun. Gages were cemented on the outer surface of the gun at several locations in order to determine chamber pressure, piston velocity, and pressures in the central breech. The high-pressure transition section deformed plastically in most rounds, and a method is suggested for estimating maximum pressures from strain-time records. Results are given for various helium pressures and powder charges.

DD FORM 1 NOV 68 1473 REPLACES DD FORM 1473, 1 JAN 64, WHICH IS OBSOLETE FOR ARMY USE.

UNCLASSIFIED

Security Classification

14. KEY WORDS	LINK A		LINK B		LINK C	
	ROLE	WT	ROLE	WT	ROLE	WT
Strain Gages Ballistic Pressures Light Gas Guns Experimental Mechanics						